

Raman scattering spectra of a superconducting $\text{Pb}_2\text{Sr}_2\text{Y}_{0.75}\text{Ca}_{0.25}\text{Cu}_3\text{O}_{8+\delta}$ single crystal

Ran Liu, M. Cardona, B. Gegenheimer, E. T. Heyen, and C. Thomsen

Max-Planck-Institut für Festkörperforschung, Heisenbergstrasse 1, D-7000 Stuttgart 80, Federal Republic of Germany

(Received 21 April 1989)

Raman spectra of a superconducting $\text{Pb}_2\text{Sr}_2\text{Y}_{0.75}\text{Ca}_{0.25}\text{Cu}_3\text{O}_{8+\delta}$ single crystal ($T_c \approx 20$ K) have been measured at different temperatures between 10 and 300 K. Through their polarization properties, the Raman features observed at 90, 150, 240, 430, 480, and 570 cm^{-1} are identified as the six A_g modes, while the mode positioned at 325 cm^{-1} has B_{1g} symmetry. The components of the Raman tensor for these phonons have been determined. The frequencies and assignments obtained here correlate well with lattice-dynamical calculations for $\text{Bi}_2\text{Sr}_2\text{CaCu}_2\text{O}_8$. The possible effect of the distortion of the oxygen atom from the ideal rocksalt-type structure of the PbO layers is discussed.

The recently discovered superconducting system $\text{Pb}_2\text{Sr}_2\text{Y}_{1-x}\text{Ca}_x\text{Cu}_3\text{O}_{8+\delta}$ with the highest T_c near 77 K has added a new family to the copper-oxide-based high- T_c superconductors.^{1,2} These compounds have a distinct crystal structure, which, nevertheless, is similar to that of $\text{RBA}_2\text{Cu}_3\text{O}_{7-\delta}$ and $(\text{Bi},\text{Tl})_2(\text{Sr},\text{Ba})_2\text{CaCu}_2\text{O}_8$ systems: A pair of CuO_2 layers separated by (R,Ca) atoms is sandwiched between (Sr,Ba)O layers. The remaining PbO and Cu layers in the $\text{Pb}_2\text{Sr}_2(\text{R},\text{Ca})\text{Cu}_3\text{O}_8$ unit cell can be regarded as a combination of the (Bi,Tl)O layers in $(\text{Bi},\text{Tl})_2(\text{Sr},\text{Ba})_2\text{CaCu}_2\text{O}_8$ and the Cu layer in $\text{RBA}_2\text{Cu}_3\text{O}_6$. In addition, it has been revealed by recent neutron-powder-diffraction³ and single-crystal x-ray-diffraction² studies that the orthorhombic symmetry distortion of these materials originates from the displacement of the oxygen atoms of the PbO planes with respect to the local rocksalt-type structural position, similar to the case of the BiO layer in $\text{Bi}_2\text{Sr}_2\text{CaCu}_2\text{O}_8$.⁴ Through consideration of these similarities in crystal structure, some insight can be gained in identifying the phonon modes as well as in understanding the superconductivity mechanism. In a previous paper,⁵ we reported Raman and infrared spectra of ceramic $\text{Pb}_2\text{Sr}_2(\text{R},\text{Ca})\text{Cu}_3\text{O}_{8+\delta}$ samples with $R = \text{Y}, \text{Eu}, \text{Sm},$ and Pr . The six prominent Raman lines at 87, 152, 238, 430, 481, and 570 cm^{-1} for $R = \text{Y}$, were tentatively assigned to vibrations of specific atoms and symmetry character, the B_{1g} mode being definitely identified by means of its characteristic depolarization ratio which shows up even in spectra of polycrystalline materials. The weak feature around 180 cm^{-1} remained unclear. In this work, we present polarized Raman spectra of single-crystal $\text{Pb}_2\text{Sr}_2\text{Y}_{0.75}\text{Ca}_{0.25}\text{Cu}_3\text{O}_{8+\delta}$. The vibrational modes are assigned to somewhat more complicated eigenvectors based on the lattice-dynamical results for $\text{Bi}_2\text{Sr}_2\text{CaCu}_2\text{O}_8$ of Ref. 6. The components of the Raman tensors for these phonons are also given. The origin of the additional feature at 180 cm^{-1} , which becomes stronger at low temperatures, is discussed.

For simplicity, the pseudotetragonal primitive cell of the undoped $\text{Pb}_2\text{Sr}_2\text{RCu}_3\text{O}_8$ is shown in Fig. 1. The structure is actually orthorhombic with space-group $Cmmm(D_{2h}^{19})$ as determined by x-ray¹ and neutron³

scattering. The motion of the R and Cu(1) atoms, which have the full symmetry of the $mmm(D_{2h})$ point group, only yields ir-active modes. All other atoms are paired with respect to the inversion through the location of R or Cu(1). These pairs lead to mutually exclusive odd (ir-active or silent) and even (Raman-active) modes (Davydov pairs).⁷ The Raman-active modes of $\text{RBA}_2\text{Cu}_3\text{O}_7$, $5A_g + 5B_{2g} + 5B_{3g}$,⁸ which have been attributed to the vibrations of five such pairs, have their equivalents also in the $\text{Pb}_2\text{Sr}_2\text{RCu}_3\text{O}_8$ structure. The remaining Raman-

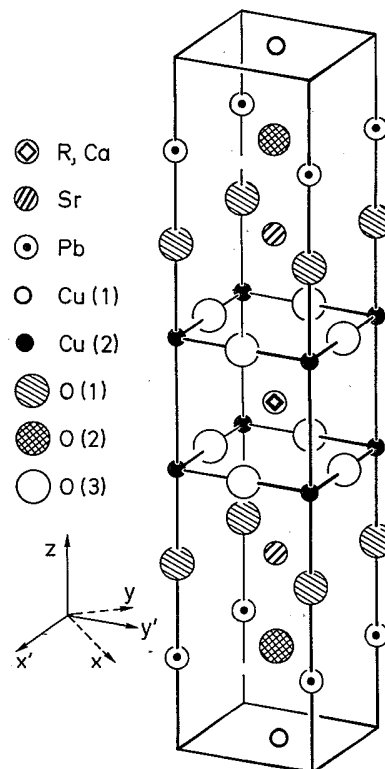


FIG. 1. Pseudotetragonal unit cell with O(2) at the ideal rocksaltlike structural position. The true orthorhombic cell has unit vectors \hat{x}, \hat{y} rotated by 45° with respect to \hat{x}', \hat{y}' .

active modes of this structure, which arise from the symmetric vibrations of Pb and O(2) pairs, can be figured out easily if the PbO plane is considered to have the ideal "rocksalt" structure: Only three modes $A_g + B_{2g} + B_{3g}$ need to be added for each of the Pb and O(2) atoms. Finally, due to the rotation of the basis vectors in this structure by 45° with respect to those of $R\text{Ba}_2\text{Cu}_3\text{O}_7$, the symmetry of one A_g mode changes into B_{1g} .⁹ In the $R\text{Ba}_2\text{Cu}_3\text{O}_7$ structure, this mode has A_g orthorhombic symmetry, although its symmetry is close to B_{1g} of the approximate tetragonal structure. The total Raman-active modes are thus $6A_g + B_{1g} + 7B_{2g} + 7B_{3g}$, which are the same as those for $(\text{Bi,Tl})_2(\text{Sr,Ba})_2\text{CaCu}_2\text{O}_8$ in the rocksalt-structure approximation for the (Bi,Tl)O layers. The B_{2g} and B_{3g} modes in the high- T_c copper oxides seem to be too weak to be unambiguously observed. This is also the case for these new compounds. Similar to the (Bi,Tl)-based compounds,⁴ some complications seem to arise from the displacement of the O(2) in the PbO plane with respect to the ideal 0,0,z position of the $Cmmm$ space group.^{2,3} This local distortion lowers the symmetry and may introduce additional Raman modes. Similarly, doping by Ca in the R position may lift some of the strict rules, especially k conservation.

Single crystals of $\text{Pb}_2\text{Sr}_2\text{Y}_{0.75}\text{Ca}_{0.25}\text{Cu}_3\text{O}_{8+\delta}$ were grown from a PbO-CuO flux. We used a precursor technique as described by Cava *et al.*¹ Platelike orthorhombic crystals up to $2.5 \times 2.5 \times 0.5 \text{ mm}^3$ dimensions with lattice parameters $a = 5.371(6)$, $b = 5.457(6)$, and $c = 15.708(2)$ Å, and with T_c of about 20 K were formed. The c axis was found to be perpendicular to the large crystal surface, and the morphological edges of the specimen ran in the [110] or $[\bar{1}\bar{1}0]$ directions referred to the orthorhombic crystallographic axes (these directions are the pseudotetragonal x' and y' axes in Fig. 1). Under polarized light (Nomarski differential interference contrast microscope) fine twin boundaries were observed in some regions of the sample surface. Polarization-dependent backscattering Raman measurements were performed at different temperatures on the untwinned region of the sample surface, where the orientation of the crystal axes (a, b) was determined by x-ray diffraction. The Raman spectra were taken with the lines of argon and krypton lasers. Some resonance behavior of the phonons was observed as well and will be presented elsewhere.¹⁰

Figure 2 shows polarized Raman spectra taken at 80 K for the $\text{Pb}_2\text{Sr}_2\text{Y}_{0.75}\text{Ca}_{0.25}\text{Cu}_3\text{O}_{8+\delta}$ single crystal with incident and scattered light propagating along the c axis (z direction). Scattering features are observed in the spectra with the incident and scattered light polarized both parallel to the pseudotetragonal crystal axis x' (or y') at 90, 152, 180, 250, 325, 430, 484, and 570 cm^{-1} . All these peaks, except the one at 325 cm^{-1} , were also observed for (x,x) and for (y,y) configurations. Most of the features, in contrast to those of the Bi-based compounds,¹¹⁻¹⁴ are quite sharp, which might be due to the possible absence of incommensurate structural modulation in the case of Pb compounds.¹⁵ The frequencies of these peaks coincide with those observed in the ceramic samples,⁵ but the weak structures around 180 cm^{-1} become much stronger at low temperatures. No peaks appear in the depolarized spec-

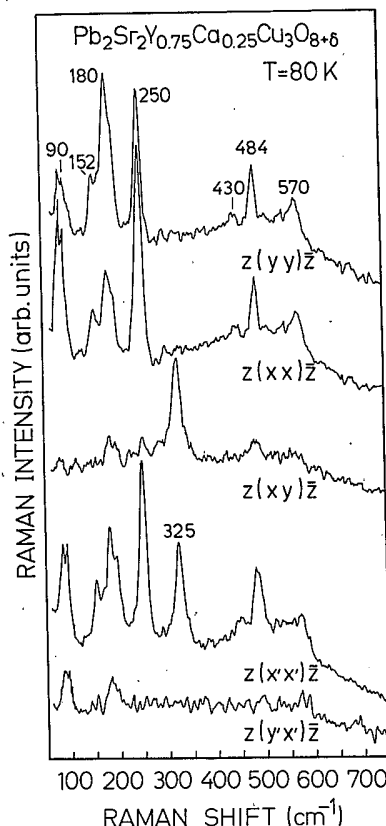


FIG. 2. Raman spectra of single-crystal $\text{Pb}_2\text{Sr}_2\text{Y}_{0.75}\text{Ca}_{0.25}\text{Cu}_3\text{O}_{8+\delta}$ taken with $k_z \parallel k_s \parallel c$, $\lambda_{\text{laser}} = 5145 \text{ \AA}$ at $T = 80 \text{ K}$.

trum $z(x',y')\bar{z}$, thus all the modes observed in this configuration have A_g or B_{1g} symmetry. The B_{1g} mode can be uniquely determined to be that at 325 cm^{-1} since only this peak also appears in $z(xy)\bar{z}$ geometry. Furthermore, the difference in the intensities of some peaks between $z(xx)\bar{z}$, $z(yy)\bar{z}$ spectra shows an obvious a - b anisotropy for the phonons around 90, 180, and 250 cm^{-1} . The polarized spectra at 295 K with incident and scattered light propagating along the x' (or y') axis are shown in Fig. 3. The peak at 570 cm^{-1} is strongly polarized in the z direction like the 500-cm^{-1} peak of $\text{YBa}_2\text{Cu}_3\text{O}_{7-\delta}$,¹⁶ the 620-cm^{-1} peak of $\text{Bi}_2\text{Sr}_2\text{CaCu}_2\text{O}_8$ (Ref. 17), and the 599-cm^{-1} peak of $\text{Tl}_2\text{Ba}_2\text{CaCu}_2\text{O}_8$.^{17,18} The spectra taken under crossed polarizations $y'z$ or $x'z$ (not shown here) show no resolvable peaks, a fact which confirms the weak Raman intensities of the B_{2g} and B_{3g} modes. The spectrum $x'(y'y')\bar{x}'$ [or $y'(x'x')\bar{y}'$] looks similar to that in $z(x'x')\bar{z}$ configuration at room temperature. Based on the polarization-dependent spectra, the components of the Raman tensors have been determined approximately and are listed in Table I.

Since the crystal structures of $\text{Pb}_2\text{Sr}_2\text{RCu}_3\text{O}_8$ and $\text{Bi}_2\text{Sr}_2\text{CaCu}_2\text{O}_8$ are quite similar, especially for the atoms involved in Raman-active modes, mode assignments may be based on existing eigenvector calculations for $\text{Bi}_2\text{Sr}_2\text{CaCu}_2\text{O}_8$.⁶ Calculations of the lattice dynamics of $\text{Pb}_2\text{Sr}_2(\text{R,Ca})\text{Cu}_3\text{O}_{8+\delta}$ are currently in progress.¹⁹ The ordering of the mode frequencies calculated in Ref. 6 is in good agreement with our assignments for ceramic sam-

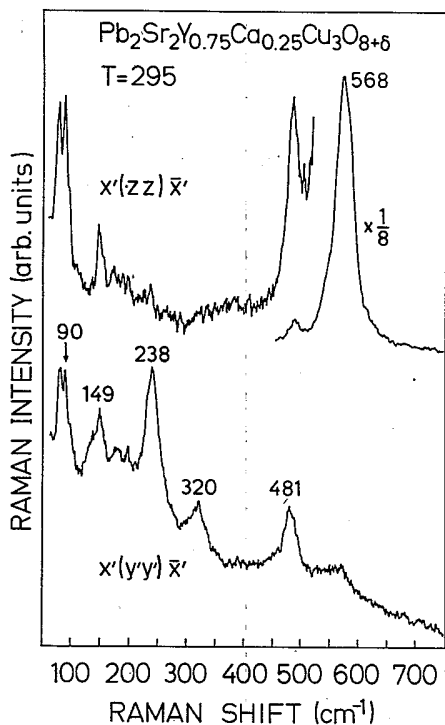


FIG. 3. Raman spectra taken with $\mathbf{k}_i \parallel \mathbf{k}_s \parallel \mathbf{x}'$, $\lambda_{\text{laser}} = 5145 \text{ \AA}$ at $T = 295 \text{ K}$.

ples⁵ if we replace Bi with Pb. The calculated modes have, however, more complicated, mixed eigenvectors, as corresponds to the behavior of complex lattices.

The mode with the lowest frequency should mainly involve the motion of the heaviest atom, Pb. The observed frequency of this mode, 90 cm^{-1} , agrees well with the theoretical estimate (87 cm^{-1}). It should be noted that the eigenvector of this mode includes also the symmetric vibrations of all other atom pairs except O(3).⁶ This phonon shows a remarkable anisotropy in the xy plane with the components of the Raman tensor roughly $\alpha_{xx} \approx \sqrt{3}\alpha_{yy}$, which is expected from the irregular coordination requirement of the Pb^{2+} .^{2,3} In addition, a closely located peak at 81 cm^{-1} may result from the existence of a

long and a short Pb—O bond in the PbO planes after distortion of O(2).

The Raman modes at 152 and 250 cm^{-1} most likely involve the vibrations of Cu(2) and Sr. According to the calculations,⁶ they should belong to in-phase and out-of-phase vibrations of Cu(2) and Sr atoms. By cooling the sample from 295 to 10 K , the frequency of the latter peak shifted by 10 cm^{-1} upwards, the width became narrower, and the anisotropy increased.

The mode at 325 cm^{-1} shows B_{1g} symmetry and it must therefore correspond to the out-of-phase bond-bending vibration of O(3). The in-phase vibration of the same atoms gives rise to the A_g mode at 430 cm^{-1} . Not only are the frequencies of these two modes about the same as the corresponding ones in $\text{YBa}_2\text{Cu}_3\text{O}_7$,^{7,8,16} but our data for ceramic samples⁵ also show a similar dependence of the B_{1g} frequency on the ionic radius of the rare-earth element.⁷ We would like to point out the experimentally observed fact that the B_{1g} -type mode is generally weak when the double CuO_2 layers are separated by Ca as compared to a rare-earth element. (A possible exception is $\text{Pb}_2\text{Sr}_2\text{DyCu}_3\text{O}_8$ for which Krol has not observed the B_{1g} peaks.²⁰) A possible explanation is found if the change in polarizability caused by the B_{1g} vibration is attributed mainly to the wave-function overlap between the oxygen atoms in the CuO_2 planes and the R or Ca atom. We would then expect a stronger Raman signal for the case of a rare earth, in which the f electrons in the outermost shell (or the d electron in the case of Y) have lower energies and higher degeneracy and, thus, should lead to higher polarizabilities than those of s electrons in Ca. In addition, less rippled CuO_2 layers found usually for the Ca centered structure might weaken the B_{1g} Raman signal through decreasing the bond-bending effect on the polarizability of the Cu—O bond. The B_{1g} mode is of special interest because of its anomalous softening below T_c in $\text{YBa}_2\text{Cu}_3\text{O}_{7-\delta}$.^{9,19,21-23} This anomaly was not observed unambiguously (although there was some indication of it) in the crystal studied here, possibly because of the low T_c (20 K) and the laser heating effect.

In the high-frequency range of the spectra, only bond-stretching vibrational modes of the oxygen atoms are involved. In A_g symmetry, these modes are vibrations of O(1) and O(2) along the z direction. In previous assign-

TABLE I. Frequencies, symmetries, assignments, and components of the Raman tensors of the Raman modes in $\text{Pb}_2\text{Sr}_2\text{Y}_{0.75}\text{Ca}_{0.25}\text{Cu}_3\text{O}_{8+\delta}$. No correction for different absorption and reflection in the different polarizations has been made.

Frequencies	Symmetries	Assignments	Components of the Raman tensors
90	A_g	Pb, Sr, Cu(2), O(1), O(2)	$\alpha_{xx} \approx \sqrt{3}\alpha_{yy}$, $\alpha_{zz} \approx \sqrt{5}\alpha_{xx}$
150	A_g	Sr, Cu(2) in phase	$\alpha_{xx} \approx \alpha_{yy}$, $\alpha_{zz} \approx \sqrt{2}\alpha_{xx}$
180	A_g^a	O(2) in-plane bending	$\alpha_{xx} \approx (\frac{2}{3})^{1/2}\alpha_{yy}$, $\alpha_{zz} \approx \alpha_{xx}$ ($T=80 \text{ K}$)
240	A_g	Sr, Cu(2) out of phase	$\alpha_{xx} \approx (\frac{2}{3})^{1/2}\alpha_{yy} \gg \alpha_{zz}$ ($T=80 \text{ K}$)
325	B_{1g}	O(3) out of phase	$\alpha_{xy} = \alpha_{yx}$, $\alpha_{zz} = 0$
430	A_g	O(3) in phase	$\alpha_{xx} \approx \alpha_{yy}$
480	A_g	O(1), O(2) in phase	$\alpha_{xx} \approx \alpha_{yy}$, $\alpha_{zz} \approx 2\alpha_{xx}$
570	A_g	O(1), O(2) out of phase	$\alpha_{xx} \approx \alpha_{yy} \ll \alpha_{zz}$

^a Not an A_g eigenmode in the ideal structure, but observed to behave as A_g .

ments,⁵ the peaks at 480 and 570 cm⁻¹ were attributed to the stretching modes of O(2) and O(1) separately. Guided by the theoretical results,⁶ we assign here these two modes to the in-phase (480 cm⁻¹) and out-of-phase (570 cm⁻¹) stretching vibrations of O(1) and O(2). The two modes around 465 and 625 cm⁻¹ in Bi₂Sr₂CaCu₂O₈ (Refs. 11-13 and 17) and around 495 and 600 cm⁻¹ in Tl₂Ba₂CaCu₂O₈ should have the same origin as the 480- and 570-cm⁻¹ modes discussed above.

The strength of the Raman mode at 180 cm⁻¹ was strongly enhanced upon cooling the sample, and from a hardly resolved spectral structure at room temperature, turned into one of the dominant peaks at low temperature. This mode has A_g symmetry with orthorhombic anisotropy $a_{xx} \approx (\frac{2}{3})^{1/2} a_{yy} \gg a_{zz}$ at 80 K. The assignment of this mode is rather difficult because we have exhausted all the eigenmodes of A_g symmetry for the "ideal" structure. Local symmetry breaking by the atomic displacement of O(2) should give rise to more Raman modes of the PbO

plane. Here, we attribute this mode tentatively to the in-plane bond-bending vibration of O(2), which is consistent with the large *ab*-plane anisotropy of this peak. The enhancement in its intensity at low temperature might be due to the ordering of the occupation of one O(2) at the four possible positions after distortion.

In conclusion, single-crystal Raman scattering measurements were performed at different temperatures. The Raman selection rules were obtained by measuring polarization-dependent spectra, and the assignment of these modes was made by comparison with early Raman experiments as well as lattice dynamical investigations of $R\text{Ba}_2\text{Cu}_3\text{O}_{7-\delta}$ and $(\text{Bi,Tl})_2(\text{Sr,Ba})_2\text{CaCu}_2\text{O}_8$ systems. The possible influence of the atomic distortion in the PbO plane on the Raman spectra has also been discussed.

We are pleased to thank K. Peters for the x-ray diffraction characterization of the crystal, and H. Hirt, M. Siemers, and P. Wurster for technical help.

- ¹R. J. Cava, B. Battlog, J. J. Krajewski, L. W. Rupp, L. F. Schneemeyer, T. Siegrist, R. B. van Dover, P. Marsh, W. F. Peck, Jr., P. K. Callaghan, S. H. Gharum, J. H. Marshall, R. C. Farrow, J. V. Waszczak, R. Hull, and P. Trevor, *Nature* (London) **336**, 211 (1988).
- ²M. A. Subramanian, J. Gopalakrishnan, C. C. Torardi, P. L. Gai, E. D. Boyes, T. R. Askew, R. B. Flippin, W. E. Farneth, and A. W. Sleight, *Physica C* **157**, 124 (1989).
- ³R. J. Cava, M. Marezio, J. J. Krajewski, W. F. Peck, Jr., A. Santoro, and F. Beech, *Physica C* **157**, 272 (1989).
- ⁴P. Bordet, J. J. Capponi, C. Chaillout, J. Chenavas, A. W. Hewat, E. A. Hewat, J. L. Hodeau, M. Marezio, J. L. Tholence, and D. Tranqui, *Physica C* **156**, 189 (1988).
- ⁵C. Thomsen, M. Cardona, R. Liu, H. J. Mattausch, W. König, F. García-Alvarado, B. Suárez, E. Morán, and M. Alario-Franco, *Solid State Commun.* **69**, 857 (1989).
- ⁶J. Prade, A. D. Kulkarni, F. W. de Wette, U. Schröder, and W. Kress, *Phys. Rev. B* **39**, 27771 (1989).
- ⁷M. Cardona, R. Liu, C. Thomsen, M. Bauer, L. Genzel, A. Wittlin, U. Amador, M. Barahona, F. Fernández. C. Otero, and R. Sáiz, *Solid State Commun.* **65**, 71 (1988).
- ⁸R. Liu, R. Merlin, M. Cardona, H. J. Mattausch, W. Bauhofer, A. Simon, F. García-Alvarado, E. Morán, M. Vallet, J. M. González-Calbet, and M. A. Alario, *Solid State Commun.* **63**, 839 (1987).
- ⁹C. Thomsen and M. Cardona, in *The Physical Properties of High-T_c Superconductors*, edited by D. M. Ginsberg (World Scientific, Singapore, 1989).
- ¹⁰E. T. Heyen *et al.* (to be published).
- ¹¹M. Cardona, C. Thomsen, R. Liu, H. G. von Schnering, M. Hartweg, Y. F. Yan, and Z. X. Zhao, *Solid State Commun.* **66**, 1225 (1988).
- ¹²G. Burns, G. V. Chandrashekar, F. H. Dacol, M. W. Shafer, and P. Strobel, *Solid State Commun.* **67**, 603 (1988).
- ¹³M. Stavola, D. M. Krol, L. F. Schneemeyer, S. A. Sunshine, R. M. Fleming, J. V. Waszczak, and S. G. Kosinski, *Phys. Rev. B* **38**, 5110 (1988).
- ¹⁴D. Kirillov, I. Bozovic, T. H. Geballe, A. Kapitulnik, and D. B. Mitzi, *Phys. Rev. B* **38**, 11955 (1988).
- ¹⁵E. A. Hewat, J. J. Capponi, R. J. Cava, C. Chaillout, M. Marezio, and J. L. Tholence, *Physica C* **157**, 509 (1989).
- ¹⁶R. Liu, C. Thomsen, W. Kress, M. Cardona, B. Gegenheimer, F. W. de Wette, J. Prade, A. D. Kulkarni, and W. Schröder, *Phys. Rev. B* **37**, 7971 (1988).
- ¹⁷R. Liu (unpublished).
- ¹⁸K. F. McCarty, B. Morosin, D. S. Ginley, and D. R. Boehme, *Physica C* **157**, 135 (1989).
- ¹⁹W. Kress, U. Schröder, J. Prade, A. D. Kulkarni, and F. W. de Wette (unpublished).
- ²⁰D. M. Krol (private communication).
- ²¹C. Thomsen, M. Cardona, B. Gegenheimer, R. Liu, and A. Simon, *Phys. Rev. B* **37**, 9860 (1988).
- ²²T. Ruf, C. Thomsen, R. Liu, and M. Cardona, *Phys. Rev. B* **38**, 11985 (1988).
- ²³M. Krantz, H. J. Rosen, R. M. Macfarlane, and V. Y. Lee, *Phys. Rev. B* **38**, 4992 (1988).